Med Biol Eng Comput (2010) 48:399–405
DOI 10.1007/s11517-010-0589-y

TECHNICAL NOTE

Enhancing the deceleration capacity index of heart rate by modified-phase-rectified signal averaging

Qing Pan · Yuexian Gong · Shijin Gong · Qijun Hu · Zhaocai Zhang · Jing Yan · Gangmin Ning

Received: 7 December 2009 / Accepted: 31 January 2010 / Published online: 6 March 2010

Abstract Deceleration capacity (DC) of heart rate is a novel indicator of autonomic nervous system (ANS) activity. In this paper, we proposed a modified DC index based on improved phase-rectified signal averaging (PRSA) algorithm. Sinusoidal analysis is applied to elucidate the rationality of the improved PRSA. Then the validity of the modified DC is verified by the databases of chronic heart failure (CHF) patients and control group. Both the conventional and modified DCs are significantly lower in CHF patients than that in the control group (2.12 ± 2.98 vs. 6.34 ± 1.92 ms, $P < 0.0001$ and 5.45 ± 2.48 vs. 10.64 ± 1.76 ms, $P < 0.0001$, respectively). And the modified DC provides higher accuracy in distinguishing CHF than the conventional one (87.4 vs. 82.1%). The results indicate that the suggested technique enhances the performance of PRSA and improves the efficiency of DC in assessing ANS activity in CHF patients.

Keywords Deceleration capacity · Phase-rectified signal averaging · Chronic heart failure

Q. Pan · Y. Gong · Q. Hu · G. Ning (✉)
Department of Biomedical Engineering, Zhejiang University, Key Laboratory of Biomedical Engineering of MOE (Yuquan Campus), Zheda Road 38, 310027 Hangzhou, China
e-mail: gmning@zju.edu.cn

S. Gong · Z. Zhang · J. Yan (✉)
Department of ICU, Zhejiang Hospital, Lingyin Road 12, 310030 Hangzhou, China
e-mail: zjicu@vip.163.com

1 Introduction

Chronic heart failure (CHF) remains a worldwide health problem which does serious harm to human health [10]. Sympathovagal imbalance in autonomic nervous system (ANS) is frequently observed in CHF patients and the measurement of ANS is helpful for the prognosis and diagnosis of CHF [11, 12, 17]. Heart rate variability (HRV) is modulated by sympathetic and vagal functions and its analysis is a kind of non-invasive tools to assess the activity of ANS [18]. Numerous studies have demonstrated that a decrease in vagal function is associated with poor prognosis in CHF patients [9, 13, 14]. Recently, a novel index termed deceleration capacity (DC) of heart rate was proposed to measure the cardiac vagal modulation [1]. The strong capability of DC in predicting mortality in patients after myocardial infarction (MI) has been reported [1, 3].

DC calculation is based on a novel technique phase-rectified signal averaging (PRSA) [2, 7]. This technique allows eliminating noises and obtaining the quasi-periodic oscillations from non-stationary signals by phase rectification and signal averaging. In the PRSA processing the phase rectification has a vital role. The aim of the present study is to propose a modified-PRSA algorithm based on the improved phase rectification and assess its potency in DC calculation.

2 Methods

In this section, the PRSA algorithm is introduced briefly and the problems in anchor point selection are addressed. A sinusoidal analysis is utilized for illustrating the influence of the phase difference on the quality of PRSA. Then, a modified DC is proposed and its efficiency is verified by a

set of databases including a CHF patient group and a control group.

2.1 DC calculation and anchor points in PRSA

DC is computed based on RR intervals derived from 24-h ECG recordings. For DC calculation, identifying the quasi-periodic components in RR intervals is required. For this purpose, PRSA algorithm is applied as follows [1]. First, RR intervals which are longer than the preceding one are selected as anchor points. In other words, for anchor point i, the RR interval RRI_i satisfies

$$\mathrm{RRI}_i > \mathrm{RRI}_{i-1}, \tag{1}$$

where $\mathrm{RRI}_{i\text{-}1}$ is the preceding RR interval. Second, RR interval segments of length $2L + 1$ are defined around each anchor point, where L should be longer than the period of the slowest fluctuation in the signal. Third, all the defined segments are centered at the anchor points and averaged. The average is given as $X(i)$, with $i = -L, -L+1, \ldots, 0, \ldots, L\text{-}1, L$, and $i = 0$ denotes the position of the anchor points. Finally, DC is derived by the equation

$$\mathrm{DC} = [X(0) + X(1) - X(-1) - X(-2)]/4. \tag{2}$$

The anchor points selected according to (1) are expected to have the same phases [2]. The averaging of the data segments is synchronized by anchor points so that the internal quasi-periodic components are enhanced and the non-stationary parts in the signals are diminished.

However, not all the anchor points are well synchronized. In general, the anchor points could be categorized into two types by their locations, as illustrated in Fig. 1.

Type I: locating on the rising edge of RR series (indicated by circle in Fig. 1), and satisfying

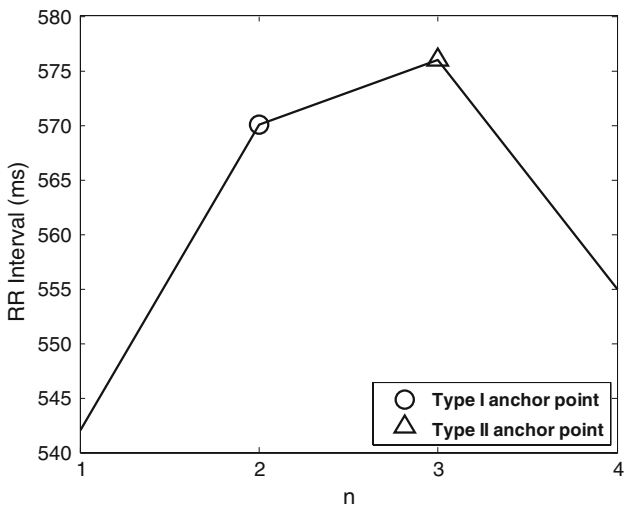

Fig. 1 Anchor points and RR intervals acquired from a section of 24-h ECG recording. The anchor points are categorized as type I (indicated by *circle*) and type II (indicated by *triangle*)

$$\mathrm{RRI}_{i+1} > \mathrm{RRI}_i > \mathrm{RRI}_{i-1}. \tag{3}$$

Type II: locating on the top of RR series (indicated by triangle in Fig. 1), and satisfying

$$\mathrm{RRI}_i > \mathrm{RRI}_{i-1}, \text{ and } \mathrm{RRI}_i > \mathrm{RRI}_{i+1}. \tag{4}$$

The type I anchor points are sure to indicate an increasing trend while the type II anchor points are uncertain to be on increasing or decreasing trend. Hence, it remains the doubt that if type II anchor points influence the outcome of PRSA processing and further DC.

2.2 Sinusoidal analysis in PRSA

For investigating the effect of type II anchor points on the outcome of PRSA in quantity, it is needed to know the exact phases of the analyzed signal. However, it is difficult to acquire the exact phases of RR interval signal. Lemay et al. [8] have justified that a simple sinusoid is available for assessing the ability of PRSA in detecting the periodic components in a signal. In the similar way, a sinusoidal signal analysis is employed in this study to illustrate the addressed problems and interpret the effect of anchor point selection criteria on PRSA processing.

For simplification, we only take the discrete sinusoids with rational normalized frequencies into consideration. Suppose that $x_n = \sin\left(2\pi n\frac{a}{b} + \delta\right)$, $n = 1, \ldots, N$ is a general expression of a discrete sinusoid, where δ is an initial phase and $\frac{a}{b}$ is the rational normalized frequency (a and b are integers). The values of a, b, and δ are arbitrary, and it is assumed that $a = 5$, $b = 12$, $\delta = 0.71\pi$. Because x_n has a period of b, only b successive samples of the signal are considered in the analysis. Continuous and discrete sinusoids are plotted in Fig. 2. It shows that in one period three anchor points are on the rising edges while the others appear on the decreasing edges. The diversity in the anchor point distribution leads to the uncertainty of the phases of the anchor points.

Under the criterion of anchor point selection, the phase range of an arbitrary anchor point x_{n_v} is

$$2\pi n_v \frac{a}{b} + \delta \in \left(-\frac{\pi}{2} + \frac{a\pi}{b}, \frac{\pi}{2} + \frac{a\pi}{b}\right) (\mathrm{mod} 2\pi). \tag{5}$$

Equation 5 shows that the phase difference among anchor points is no more than π and the phase of anchor points lies in $\left(-\frac{\pi}{2} + \frac{a\pi}{b}, \frac{\pi}{2} + \frac{a\pi}{b}\right)$. It implies that some anchor points may appear on the decreasing edge (with phase larger than $\frac{\pi}{2}$) and in this paper they are named as pseudo anchor points.

Due to the phase difference among anchor points, the actual PRSA average differs from the original signal in two aspects: phase shift and amplitude attenuation. For comparing the differences between the original signal and PRSA average, the PRSA average x_k is derived as

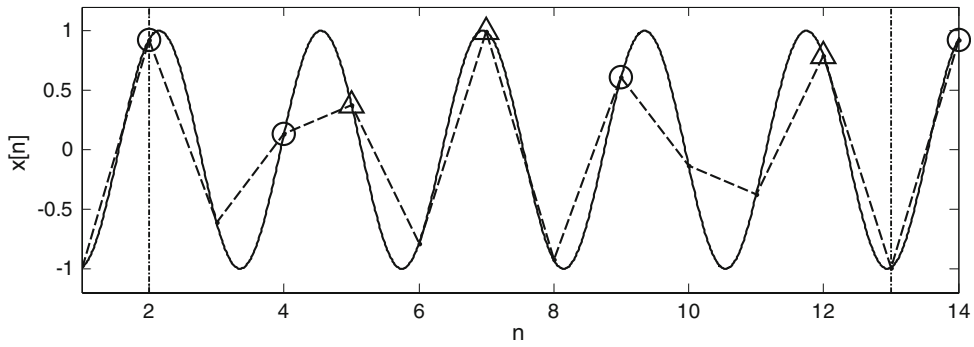

Fig. 2 Anchor points on continuous and discrete sinusoids. The *solid line* represents the continuous sinusoid and the *dash line* represents the discrete sinusoid. The anchor points on rising edges are indicated by *circle* and the ones on decreasing edges are indicated by *triangle*. One period of the sinusoid is defined by the vertical dash-dot lines

$$x_k = 2\frac{\sin(m\pi/b)\cdot\sin(\pi/b)}{m[1-\cos(2\pi/b)]} \times \sin\left(2\pi(k+k_0)+\delta+\frac{m-1}{b}\pi\right), \quad (6)$$

where m is the number of the anchor points involved in the averaging and ranges from 1 to M. k is the index of data points in the averaging and k_0 is the index of the anchor point closest to $-\frac{\pi}{2}$.

The pseudo anchor points might impose negative effects on the PRSA averaging due to their opposite phases. For verifying this, the exact phases of the anchor points in one period are analyzed. The phase of the anchor point which is closest to $-\frac{\pi}{2}$ is determined as φ. Subsequently, the phases of the anchor points are $\varphi + n\frac{2\pi}{b}$, $n = 0, 1, \ldots, M\text{-}1$, where M is the number of anchor points and it equals to the integer part of $\frac{b}{2}$ minus or plus one. The pseudo anchor points have the largest phase difference from phase φ, which are given as $\varphi + (M-1)\frac{2\pi}{b}$, $\varphi + (M-2)\frac{2\pi}{b}\ldots\varphi + (M-l)\frac{2\pi}{b}$. l is the number of pseudo anchor points. Details about the determination of l are given in the appendix. Omitting the pseudo anchor points reduces m in (6) and thus the phase shift $\frac{m-1}{b}\pi$. The phase shift approximates to zero when m is reduced toward one. The amplitude of the sinusoid in (6) is $2\frac{\sin(m\pi/b)\cdot\sin(\pi/b)}{m[1-\cos(2\pi/b)]}$ and it can be further given as $\frac{\pi}{b\sin(\pi/b)}\cdot\frac{\sin(m\pi/b)}{m\pi/b}$. Because b is a constant, only the monotonicity of $\frac{\sin(m\pi/b)}{m\pi/b}$ needs to be discussed for the signal amplitude. Since $m \in [1, M]$ and M equals the integer part of $\frac{b}{2}$ minus or plus one, the range of $m\pi/b$ is $\left(\frac{1}{b}\pi, \left(\frac{1}{2}+\frac{1}{b}\right)\pi\right)(b > 1)$, and it can be proved that the signal amplitude monotonously decreases when $m\pi/b$ is in this interval. Thus, the amplitude of the PRSA average increases with the reduction of m and equals to the original amplitude of the signal when m is reduced to one. The comparison of these two aspects suggests that removing pseudo anchor points brings about a better outcome of PRSA average.

2.3 Modified DC calculation

In DC calculation, the pseudo anchor points cannot be figured out precisely in RR interval signals. However, the occurrence of pseudo anchor points is clearly observed when RR interval series are interpolated by cubic spline method (Fig. 3). It can also be seen that the pseudo anchor points are bound to turn up on the top of the RR interval series. Consequently, omitting the anchor points on the top will eliminate the impact of pseudo anchor points and improve the performance of PRSA average.

Three different criteria of anchor point selection are applied to calculate PRSA. The corresponding PRSA averages are indicated by different subscripts:

$PRSA_{org}$, PRSA average calculated by all the anchor points according to (1);
$PRSA_{inc}$, PRSA average calculated by anchor points on the rising edge;
$PRSA_{top}$, PRSA average calculated by anchor points on the top.

Accordingly, DCs based on different criteria of anchor point selection are performed to evaluate the efficiency of the modified algorithm:

DC_{org}, DC calculated by $PRSA_{org}$;
DC_{inc}, DC calculated by $PRSA_{inc}$;
DC_{top}, DC calculated by $PRSA_{top}$.

2.4 Datasets and statistical analysis

The effect of the modified PRSA on DC is the major concern. Thus, the long term RR interval databases from PhysioNet (www.physionet.org) are analyzed. Totally 44 CHF cases serve as the CHF group. They are from two databases. One provides 29 CHF cases (8 men, 2 women, gender is unknown for the remaining 19 subjects, aged 55.0 ± 11.9, NYHA I-III). The other provides 15 severe CHF cases (11 men and 4 women, aged 56.0 ± 11.5, NYHA III-IV). Fifty-four healthy subjects (30 men and 24 women, aged 61.3 ± 11.8) are enrolled as the control group. Two subjects in the CHF group and one in the control group with excessive atrial premature beats are excluded.

The statistical results are represented as mean ± SD. The difference between any two groups is compared by

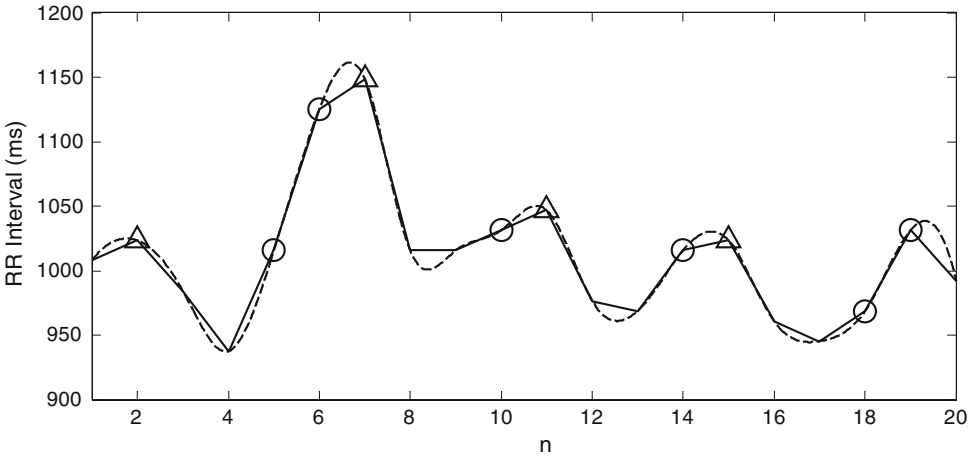

Fig. 3 The interpolation of RR intervals by cubic-spline method. The RR intervals connected by *solid line* are acquired from a section of 24-h ECG recording. The RR intervals interpolated by cubic-spline method are given as the *dash line*. The anchor points on rising edges are indicated by *circle*. The pseudo anchor points are indicated by *triangle*

Student's *t* test (normally distributed data) or Wilcoxon sign-rank test (variables not meeting normality criteria). Receiver operating characteristic (ROC) curves are calculated for DCs and proper thresholds are selected from the curves to reach a compromise between sensitivity and specificity. The accuracies in distinguishing the CHF patients under the selected thresholds are computed for DC_{org}, DC_{inc}, and DC_{top}, respectively.

3 Results

3.1 Behave of modified-PRSA curves

Typical PRSA curves under different anchor point selection criteria are illustrated in Fig. 4. The segment length L for PRSA is set to 60. Several notable patterns in PRSA curves are observed. Near the center of the curve (anchor point) a dramatic oscillation of RR interval arises and the largest one appears in $PRSA_{inc}$. The RR interval oscillations in the three PRSA curves decay from the anchor point toward the two ends and have different modes. In $PRSA_{inc}$ and $PRSA_{org}$, the decaying oscillations are modulated by low frequency, whereas in $PRSA_{top}$ although the variation of RR interval is comparable to that in $PRSA_{org}$, the low frequency modulation is not obvious. It can also be seen that the RR intervals of $PRSA_{inc}$, $PRSA_{org}$, and $PRSA_{top}$ have different levels. While $PRSA_{inc}$ has the longest mean RR interval of 743.7 ms, $PRSA_{top}$ has the shortest of 701.8 ms, and $PRSA_{org}$ has the median value of 718.3 ms. Further exploration indicates that the levels of RR intervals in PRSA curves are related to the distribution of anchor points over the data series. For a data section with longer RR intervals, the anchor points are prone to be located on the rising edge. In contrast, for shorter RR interval series, the anchor points appear more likely on the top.

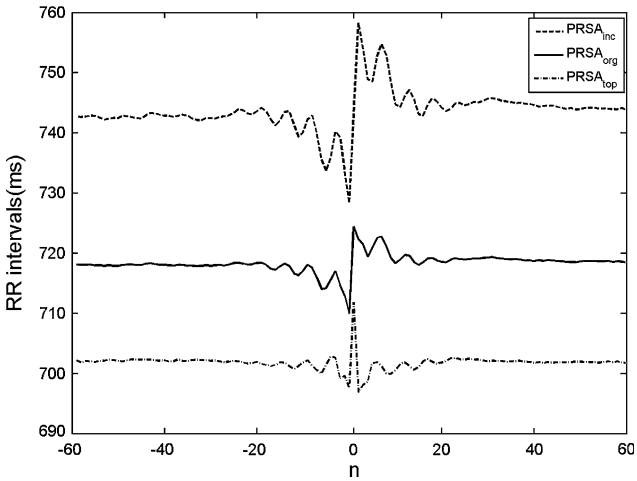

Fig. 4 The PRSA curves obtained by different criteria of anchor point selection. The segment length of PRSA curves is 60. $PRSA_{org}$: PRSA calculated by all the anchor points. $PRSA_{inc}$: PRSA calculated by anchor points on rising edges. $PRSA_{top}$: PRSA calculated by anchor points on tops

3.2 Performance of DC

DC values under different rules of anchor point selection are calculated for the control group and the CHF group and the results are given in Table 1. The mean values of DC_{org}, DC_{inc}, and DC_{top} for the control group are 6.34 ± 1.92, 10.64 ± 1.76, and 3.35 ± 1.21 ms, respectively. And the corresponding DC values for the CHF group are

Table 1 DCs for CHF and control group

	CHF	Control	*P*-value
DC_{org}(ms)	2.12 ± 2.98	6.34 ± 1.92	<0.0001
DC_{inc}(ms)	5.45 ± 2.48	10.64 ± 1.76	<0.0001
DC_{top}(ms)	1.13 ± 1.96	3.35 ± 1.21	<0.0001

2.12 ± 2.98, 5.45 ± 2.48, and 1.13 ± 1.96 ms, respectively. In contrast to the control group, the values of DCs in the CHF group are significantly lower. In both groups, DC_{inc} is the highest, and DC_{top} is the lowest among the DC indices.

For distinguishing CHF by DCs, the thresholds are determined as 4.81, 8.59, and 2.75 ms for DC_{org}, DC_{inc}, and DC_{top}, respectively. Under the selected thresholds, in total 95 cases, 78, 83, and 73 cases are correctly classified by DC_{org}, DC_{inc}, and DC_{top}, with accuracies of 82.1, 87.4, and 76.8%, respectively. The performance of DC_{inc} is the best while DC_{top} has the lowest accuracy.

4 Discussion

In clinic, the sympathovagal imbalance of ANS, which is characterized by sympathetic overactivity and parasympathetic withdrawal, is related to poor prognosis of cardiovascular diseases. Some attempts have been made for recognizing sympathetic and vagal activities of ANS [2, 5, 15, 19]. DC is one of the most persuasive and convenient indices for this purpose, whereas the effect of anchor point selection in PRSA algorithm on the performance of DC is rarely noticed in previous studies. In this paper, we proposed a modified DC based on improved PRSA and investigated its capability in distinguishing CHF.

4.1 The performance of modified-PRSA curves

The present results indicate that the modified-PRSA better reflects the periodic components in RR interval series. The periodicity is one of the main concerns in RR interval analysis. In view of the principle of PRSA, the oscillation near the anchor point is composed of all the quasi-periodicities in the original signal [2]. The fact that $PRSA_{inc}$ has the largest oscillation near the anchor point suggests that the internal periodic components in RR intervals are enhanced due to better phase synchronization. As DC is calculated from the RR interval series near the anchor point, the prominent periodicities in $PRSA_{inc}$ further contribute to the improved ability of the modified DC in distinguishing CHF.

The data series outside the distinctive oscillation around the anchor point may also convey physiological messages. The decaying oscillation modulated by low frequency in $PRSA_{inc}$ and $PRSA_{org}$ is probably due to the compensatory mechanism of ANS which agrees with the physiological understanding of ANS regulation after the sudden change of cardiac rhythm [6]. The disappearance of the low frequency modulation in $PRSA_{top}$ implies that the regulation information is weakened by the poor synchronization of RR intervals.

4.2 The efficiency of the modified DC

Significant difference between the DC values of the CHF and healthy group (shown in Table 1) indicates that a low DC is strongly associated with CHF. The accuracies of DC_{inc}, DC_{org}, and DC_{top} in distinguishing CHF patients are 87.4, 82.1, and 76.8%, respectively. The ROC analysis demonstrates that the area under the curve (AUC) of DC_{inc} is significantly larger than that of DC_{org} (0.94 ± 0.02 vs. 0.90 ± 0.03, $P < 0.05$) and DC_{top} (0.94 ± 0.02 vs. 0.87 ± 0.04, $P < 0.05$). Although the current results need to be further verified by larger scale investigation, they clearly reveal that with the reduction of top anchor points, the accuracy of DC in distinguishing CHF is raised and the AUC is increased. Previous report stated that the LF/HF ratio of HRV has an accuracy of 72% in diagnosing heart failure [4]. In the present study, DC_{inc} demonstrates higher accuracy than the reported LF/HF index. All these findings suggest that the capability of modified DC in assessing the vagal activity is surely improved.

Furthermore, the results of DC analysis may also provide clue to a feasible ECG recording for DC calculation. The high level of RR intervals in $PRSA_{inc}$ shows that data segments selected from the resting periods that possess long RR intervals are more suitable for a reliable DC. It implies the possibility that a DC calculation could be achieved based on a short-term ECG recording in controlled resting condition instead of 24-h ECG recording. If a short-term DC is verified by further study, it would strongly prompt the application of DC in clinical practice.

In addition, the PRSA modification does not add the complexity in DC calculation and the reduction of anchor points does not lessen the efficiency of DC. As a result of the top anchor points being discarded, the number of the anchor points in 24-h ECG recordings reduces from about 40000 to 2000–15000 in the involved dataset. And a recent study has suggested that only 100–1000 points are required for a well-behaved PRSA average [16].

4.3 The limitation of the study

It is worth pointing out that as an initial work, the current study proposes a technical method more than a clinical solution for diagnosis and its possible application in clinic needs more investigations. First, the improved method is not verified by separated test and validation datasets due to the limited number of cases. It may result in the bias in assessing the classification accuracy. Second, the detailed characteristics of the patients are not given in the database. It prevents us from exploring a convinced physiological interpretation of the improved performance of DC and further the association between DC and ANS. Prospective studies with larger number of cases are needed to validate

the performance of the modified DC in the diagnosis of CHF and other cardiovascular diseases.

5 Conclusion

The present work demonstrates that the anchor points locating on the top of the signal curve may have negative effect on the phase rectification of PRSA and a modification of anchor point selection in DC calculation is proposed. The rationality of the modification is explained by a detailed theoretical analysis. Finally, it is proved that the modified DC is superior to the conventional approach in distinguishing CHF cases. The strong significance of the modified DC will encourage its application in clinic.

Acknowledgments This work is supported by the National Nature Science Foundation of China (Grant 30570483) and the Science and Technology Department of Zhejiang Province, China (Grant 2006C13018).

Appendix

A theoretical derivation is presented in the appendix for calculating the number of pseudo anchor points in one period of a discrete sinusoid.

The discrete sinusoid is given as $x_n = \sin\left(2\pi n\frac{a}{b} + \delta\right)$, $n = 1, \ldots, N$. The sample points categorized to pseudo anchor points follow two criteria:

(1) The sample points locate on the decreasing edge;
(2) Each point is larger than the former one.

The two criteria lead to a relationship among the index of the sample points, the normalized frequency and the initial phase. Phases of the points follow criterion (1) correspond to:

$$\frac{1}{2}\pi + 2k\pi < 2\pi n\frac{a}{b} + \delta < \frac{3}{2}\pi + 2k\pi. \tag{7}$$

It can be further derived as:

$$\frac{b\pi + 4kb\pi - 2\delta b}{4a\pi} < n < \frac{3b\pi + 4kb\pi - 2\delta b}{4a\pi} \tag{8}$$

and the phases of the points follow criterion (2) correspond to:

$$\sin\left(2\pi n\frac{a}{b} + \delta\right) > \sin\left(2\pi(n-1)\frac{a}{b} + \delta\right). \tag{9}$$

It can be simplified as:

$$2\cos\left(2\pi n\frac{a}{b} - \frac{a}{b}\pi + \delta\right)\sin\left(\frac{a}{b}\pi\right) > 0. \tag{10}$$

Since a and b are positive integers and $a < b$ (because b is the period of the sinusoid), the range of $\frac{a}{b}\pi$ is limited in $(0, \pi)$ and thus $\sin\left(\frac{a}{b}\pi\right) > 0$. So $\cos\left(2\pi n\frac{a}{b} - \frac{a}{b}\pi + \delta\right) > 0$. The range of the phase is given as:

$$2k\pi < 2\pi n\frac{a}{b} - \frac{a}{b}\pi + \delta < \frac{\pi}{2} + 2k\pi$$

or

$$\frac{3}{2}\pi + 2k\pi < 2\pi n\frac{a}{b} - \frac{a}{b}\pi + \delta < 2\pi + 2k\pi. \tag{11}$$

The relationship among n and a, b, δ is obtained as:

$$\frac{2kb\pi + a\pi - \delta b}{2a\pi} < n < \frac{4kb\pi + b\pi + 2a\pi - 2\delta b}{4a\pi}$$

or

$$\frac{4kb\pi + 3b\pi + 2a\pi - 2\delta b}{4a\pi} < n < \frac{2kb\pi + 2b\pi + a\pi - \delta b}{2a\pi} \tag{12}$$

In both (8) and (12), k ranges from 0 to $a-1$. In conclusion, when the index of the sample point, the normalized frequency, and the initial phase satisfy with (8) and (12), this sample point is a pseudo anchor point.

References

1. Bauer A, Kantelhardt JW, Barthel P et al (2006) Deceleration capacity of heart rate as a predictor of mortality after myocardial infarction: cohort study. Lancet 367:1674–1681
2. Bauer A, Kantelhardt JW, Bunde A et al (2006) Phase-rectified signal averaging detects quasi-periodicities in non-stationary data. Physica A 364:423–434
3. Bauer A, Barthel P, Schneider R et al (2009) Improved stratification of autonomic regulation for risk prediction in post-infarction patients with preserved left ventricular function (ISAR-Risk). Eur Heart J 30:576–583. doi:10.1093/eurheartj/ehn540
4. Bonaduce D, Petretta M, Marciano F et al (1999) Independent and incremental prognostic value of heart rate variability in patients with chronic heart failure. Am Heart J 138:273–284
5. Chen XX, Mukkamala R (2008) Selective quantification of the cardiac sympathetic and parasympathetic nervous systems by multisignal analysis of cardiorespiratory variability. Am J Physiol Heart Circ Physiol 294:H362–H371. doi:10.1152/ajpheart.01061.2007
6. Guyton AC, Hall JE (2000) Textbook of medical physiology. W. B. Saunders, Philadelphia
7. Kantelhardt JW, Bauer A, Schumann AY et al (2007) Phase-rectified signal averaging for the detection of quasi-periodicities and the prediction of cardiovascular risk. Chaos 17:015112
8. Lemay M, Prudat Y, Jacquemet V et al (2008) Phase-rectified signal averaging used to estimate the dominant frequencies in ECG signals during atrial fibrillation. IEEE Trans Biomed Eng 55:2538–2547
9. Li M, Zheng C, Sato T et al (2004) Vagal nerve stimulation markedly improves long-term survival after chronic heart failure in rats. Circulation 109:120–124. doi:10.1161/01.cir.0000105721.71640.da
10. McMurray JJV, Pfeffer MA (2005) Heart failure. Lancet 365:1877–1889
11. Miyamoto S, Fujita M, Sekiguchi H et al (2001) Effects of posture on cardiac autonomic nervous activity in patients with congestive heart failure. J Am Coll Cardiol 37:1788–1793

12. Mortara A, Tavazzi L (1996) Prognostic implications of autonomic nervous system analysis in chronic heart failure: role of heart rate variability and baroreflex sensitivity. Arch Gerontol Geriatr 23:265–275
13. Mortara A, La Rovere MT, Pinna GD et al (1997) Arterial baroreflex modulation of heart rate in chronic heart failure: clinical and hemodynamic correlates and prognostic implications. Circulation 96:3450–3458
14. Olshansky B, Sabbah HN, Hauptman PJ et al (2008) Parasympathetic nervous system and heart failure: pathophysiology and potential implications for therapy. Circulation 118:863–871. doi:10.1161/circulationaha.107.760405
15. Piskorski J, Guzik P (2007) Geometry of the poincare plot of RR intervals and its asymmetry in healthy adults. Physiol Meas 28:287–300
16. Schumann AY, Kantelhardt JW, Bauer A et al (2008) Bivariate phase-rectified signal averaging. Physica A 387:5091–5100
17. Szabo BM, van Veldhuisen DJ, vander Veer N et al (1997) Prognostic value of heart rate variability in chronic congestive heart failure secondary to idiopathic or ischemic dilated cardiomyopathy. Am J Cardiol 79:978–980
18. Task Force of the European Society of Cardiology and the North American Society of Pacing and Electrophysiology (1996) Heart rate variability: standards of measurement, physiological interpretation, and clinical use. Circulation 93:1043–1065
19. Zhong YR, Jan KM, Ju KH et al (2006) Quantifying cardiac sympathetic and parasympathetic nervous activities using principal dynamic modes analysis of heart rate variability. Am J Physiol Heart Circ Physiol 291:H1475–H1483. doi:10.1152/ajpheart.00005.2006